CHIN. PHYS. LETT. Vol. 37, No. 11 (2020) 114201

Semi-Ellipsoid Nanoarray for Angle-Independent Plasmonic Color Printing

Jiancai Xue(薛建材), Limin Lin(林丽敏), Zhang-Kai Zhou(周张凯)*, and Xue-Hua Wang(王雪华)

State Key Laboratory of Optoelectronic Materials and Technologies, School of Physics, Sun Yat-sen University, Guangzhou 510275, China

(Received 4 August 2020; accepted 9 September 2020; published online 8 November 2020)

Employing a silver nano semi-ellipsoid nanoarray with high symmetry into applications in plasmonic color printing, we fulfill printing images with colors independent of observing angles. Also, by decreasing the period of a nano semi-ellipsoid array into deep-subwavelength scales, we obtain high reflectivity over 50%, promising high efficiency for imaging generations. A facile technique based on the transfer of anodized aluminum oxide template is developed to fabricate the silver nano semi-ellipsoid nanoarray, realizing plasmonic color printing with features of low cost, scalable, full color and high flexibility. Our approach provides a feasible way to address the angle-dependent issue in the previous practice of plasmonic color printing, and boosts this field on its way to real-world commercial applications.

PACS: 42.70.−a, 73.20.Mf, 71.45.Gm, 42.25.Fx, 82.45.Cc DOI: 10.1088/0256-307X/37/11/114201

Metallic nanostructures supporting localized surface plasmon resonances possess the capability of enhancing light-matter interaction wavelength-selectively,[1−4] which leads to preferential absorption, scattering or diffraction. This phenomenon is always accompanied by generation of all kinds of vivid colors,[5−7] and has been used to create beautiful art crafts thousands of years ago, long before people know the underline mechanism. Recently, with the rapid development of nanotechnology, plasmonic nanostructures have begun to play an important role in research of next-generation color printing technology.[8−15] This field, termed as plasmonic color printing, provides several unprecedented advances such as ultrahigh resolution, non-fading colors and compatibility with multi-functionalities. In addition, compared with other advanced color printing technology, such as those based on dielectric nanostructures,[16−18] plasmonic color printing holds distinct advantages in constructing functional color devices.

With tremendous research efforts devoted, plasmonic color printing has obtained substantial progresses in many aspects regarding color gamut,[14,15,19,20] color tunability,[21−24] fabricating techniques,[25−27] and functionalization,[28−31] and so on. However, a crucial problem that has not been solved properly is the issue of angle-dependence of demonstrated colors. Most of the previous work showed angle-dependent optical responses, which is not favorable in normal daily scenarios, because normally we expect a print to appear as a consistent pattern to people standing at different angles. Many kinds of plasmonic nanostructures have been presented to reduce the influence of observing angle, including nanodimers,[32] random nanostructures,[33,34] tandem nanodisks[35] and gap-plasmonic antennas,[15] whereas these plasmonic nanostructures are restricted by either very limited color gamut, low angle-independence with angle larger than 40°, or feasibility only for particular polarizations. Regarding this issue, high-symmetric nanostructures such as metallic nanospheres may bring some inspiration. However, the direct assembling of such structures still cannot provide the optical response with angle independence.[36] Therefore, to tackle this problem, new structures should be developed for plasmonic color printing.

In this Letter, we provide a practical design of angle-independent plasmonic color printing that keeps its colors unchanged even when the incident angle is up to 60°. In the designed plasmonic nanostructures, silver nano semi-ellipsoids are arranged into a nanoarray with a deep-subwavelength period, which not only have optical features tunable from the blue region to the red region of the visible spectra, but also possess high reflective efficiency. Instead of just using semi-spheres, the utilization of semi-ellipsoids provides higher tunability regarding both peak wavelengths and generated color range. We then put the

Supported by the China Postdoctoral Science Foundation (Grant No. 2020M672957), the National Natural Science Foundation of China (Grant No. 11974437), the Guangdong Natural Science Funds for Distinguished Young Scholars (Grant No. 2017B030306007), the Guangdong Special Support Program (Grant No. 2017TQ04C487), the Pearl River S&T Nova Program of Guangzhou (Grant No. 201806010033), the Open Fund of IPOC (BUPT) (Grant No. IPOC2019A003), and the Fundamental Research Funds for the Central Universities (Grant No. 20lgzd30).

*Corresponding author. Email: zhouzhk@mail.sysu.edu.cn

© 2020 Chinese Physical Society and IOP Publishing Ltd

design into practice by a scalable technique based on transfer of anodized aluminum oxide (AAO) template, and further show flexible plasmonic color printing. Finally, the potential of functionalization with visualized sensing is discussed.

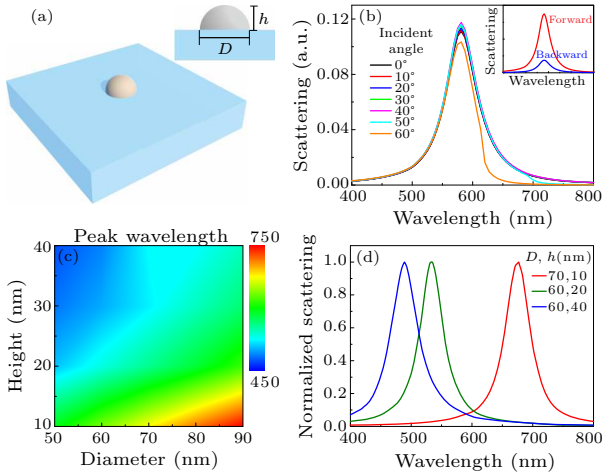

Fig. 1. Angle independence of single silver nano semi-ellipsoid on silica. (a) Schematic of a single silver nano semi-ellipsoid. (b) The scattering spectra of a silver nano semi-ellipsoid with diameter $D = 80$ nm and height $h = 20$ nm with regard to different incident angles from 0° to 60°. Inset: the forward and backward scattering spectra of the semi-ellipsoid under normal incidence. (c) The distribution of the reflective peak wavelengths of the semi-ellipsoids regarding different D and h. The data was simulated with $D = 50$, 60, 70, 80, 90 nm and $h = 10$, 20, 30, 40 nm. Other data of the peak wavelengths was obtained by interpolation. (d) The scattering spectra of three instances of semi-ellipsoids with reflective peak wavelengths located in blue, green and red regions of visible spectra, respectively. The light source used in the simulations is s-polarized.

To develop the angle-independent plasmonic color printing, the first step is to identify a structural unit that responds to light independent of incident angles. To this end, we investigate the optical responses of a highly symmetric nanostructure which is a silver nano semi-ellipsoid on a silica substrate ($n = 1.5$) demonstrated in Fig. 1(a). The symmetric morphology of the semi-ellipsoid would be physically less sensitive to incident angles of light when compared with other structures such as rods and dimers. We calculate the optical responses of structures by the finite-difference time-domain (FDTD) method,[37] and the optical refractive index was taken from Palik.[38] As an example shown in Fig. 1(b), a semi-ellipsoid [diameter $D = 80$ nm and height $h = 20$ nm] has optical response well independent of incident angles, with no obvious change of the peak wavelength in scattering when the incident angle is altered from 0° to 60°.

The resonant wavelength of the semi-ellipsoid is a tunable factor that can be modulated by changing D and h, with larger D or smaller h corresponding to longer wavelength [Fig. 1(c)]. As shown in Fig. 1(c), the resonant wavelength of the semi-ellipsoids can be altered from the blue region to the red region of the visible spectra. Using semi-ellipsoids instead of just semi-spheres ($h = D/2$), the resonant features are more tunable in a wider arrange of spectra. Figure 1(d) provides three examples of the tunable optical feature, with three sets of parameters corresponding to resonant wavelengths in blue region ($D = 60$ nm, $h = 40$ nm), green region ($D = 60$ nm, $h = 20$ nm) and red region ($D = 70$ nm, $h = 10$ nm), respectively. This feature and the angle independence introduced above together are the basis of our angle-independent plasmonic color printing.

A single nanoparticle only has quite weak influence on macroscopic light and the scattered light is mainly forward [inset in Fig. 1(b)], making it unpractical for color printing. Therefore, the arrangement way of the semi-ellipsoids should be considered. Nanoparticles distributed in a random and dispersed way can retain the angle-independent property, but the reflective efficiency would be very low,[39] which is not preferred in color printing. On the other hand, ordered arrangement with period comparable to wavelength may cause diffractive effect that is sensitive to incident angles.[40,41] To achieve high reflective efficiency while maintaining the angle-independent characteristic, we arrange silver nano semi-ellipsoids into periodic arrays of hexagonal lattice with deep-subwavelength periods ($P = 110$ nm), as shown in Fig. 2(a). The deep-subwavelength arrangement of the unit particles effectively inhibits the forward scattering and, thus, gives rise to higher reflection efficiency than the cases with larger periods [Fig. 2(b)]. The hexagonal lattice is chosen for its form of close packing arrangement, which also benefits the high reflection efficiency of the nanoarray.

Figure 2(c) shows an example of the angle-independent feature of the periodic semi-ellipsoid array, where the reflective peak wavelength of the array ($D = 80$ nm, $h = 20$ nm) has no distinct change when the incident angle is altered from 0° to 60°. The peak reflections show slight decreases when the incident angle is increased, but remain in a relative high level, larger than 50% in this case.

On the other hand, regarding angle-independent colors, one should also consider the polarization state of incident light, which is a very important factor affecting the performances of structural colors. To achieve angle-independent plasmonic color printing in real-world scenarios, the reflected color of the structures should be both angle-independent and polarization-independent. Because if the reflected colors are angle-independent only regards one polarization state, the reflected light of the other polarization would cause changes to the overall colors of the printing patterns. Fortunately, although this factor haunts many existing works on plasmonic color

printing,[11,15,19,36,42,43] it is not a problem to the semi-ellipsoid nanoarray-based printing. Due to the high symmetry of the unit structures, the optical responses of the semi-ellipsoid nanoarray under s-polarized light is in accordance with that under p-polarized light, as shown in Fig. 2(c).

As illustrated in Fig. 2(d), the modulation principle of the periodic arrays is consistent with that of single particles, i.e., larger D and smaller h result in longer peak wavelengths. Figure 2(d) shows that the reflective peak wavelength of the plasmonic array can be tuned from the blue region to the red region of the visible spectra, which brings about the capability of full color generation. This is shown more clearly by plotting the corresponding colors of the calculated arrays in the CIE color space, demonstrating the colors from blue to green and red [Fig. 2(e)]. The results in Figs. 2(d)–2(e) also demonstrate the advantages of semi-ellipsoids over semi-spheres ($h = D/2$), where the former can provide larger tuneability regarding both resonant wavelengths in spectra and colorimetric area in generated colors, while the latter can only achieve a small part of them.

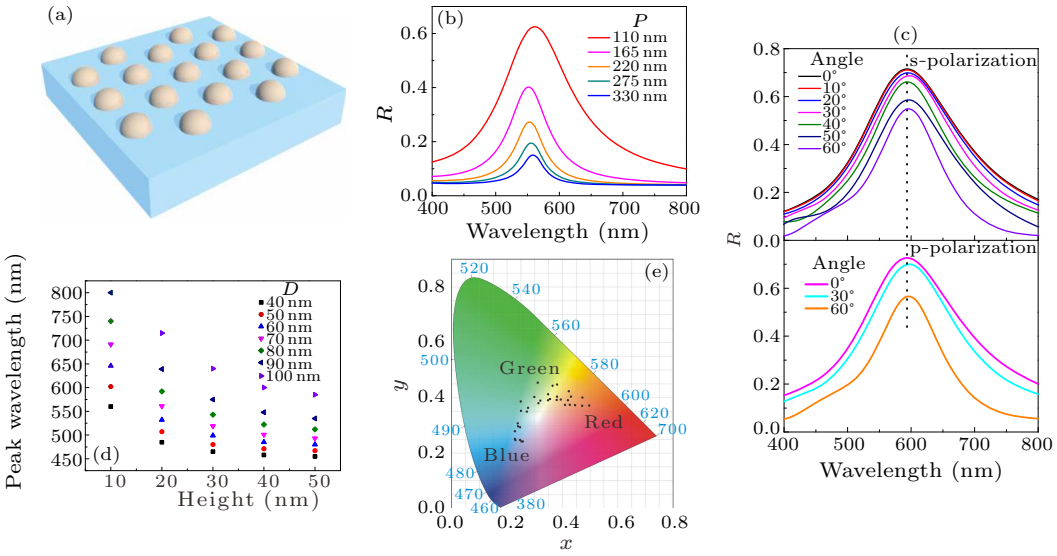

Fig. 2. Optical response of silver semi-ellipsoid nanoarray. (a) Schematic of a silver semi-ellipsoid nanoarray. (b) The simulated reflection spectra of a silver semi-ellipsoid nanoarray with periods ranging from 110 nm to 330 nm. $D = 70$ nm, $h = 20$ nm. The used light source is s-polarized. (c) The simulated reflection spectra of a silver semi-ellipsoid nanoarray with $D = 80$ nm, $h = 20$ nm and $P = 110$ nm regarding different incident angles from 0° to 60°. The used light source is s-polarized for the upper panel, and p-polarized for the lower panel. (d) The distribution of the reflective peak wavelengths of the semi-ellipsoid nanoarrays regarding different D and h. (e) The distribution of CIE xy coordinates of the colors generated by the semi-ellipsoid arrays with D ranging from 40 to 100 nm and h ranging from 10 to 50 nm, corresponding to the data in (d).

Experimentally, we used a transfer technique based on a porous AAO template[44–46] to fabricate the angle-independent plasmonic color printing. Firstly, we fabricated the AAO templates by a two-step anodization process.[47,48] Pure aluminum sheets (99.999%) were electropolished in a mixture of $HClO_4$ and C_2H_5OH with the volumetric ratio of 1 : 3 to smooth surface, at a constant current of 1.2 A and temperature of 0 ℃. Then the aluminum sheets were anodized in 0.3 M oxalic acid with a voltage of 45 V and temperature of about 4 ℃ for 6 h to form an AAO layer, which were removed in a mixture of 6 wt% phosphoric acid and 1.8 wt% chromic acid at 60 ℃ for 1.5 h. Next, new regular AAO templates were produced by anodization under the same conditions as the first anodization, but with anodizing duration of 300 s. A layer of positive-tone S1805 photoresist was spin-coated onto the as-prepared AAO template and then the predesigned pattern was printed in the photoresist by directly writing photolithography on a Heidelberg uPG501 system. The sample was subsequently developed in 2.38% TMAH to form a relief pattern in photoresist, enabling selective etching with 0.3 M oxalic acid at a temperature of 45 ℃. After the first etching, the remaining photoresist was removed by acetone at 50 ℃ for 1 h to expose all the surface of the AAO template, followed by a second etching with proper duration enlarging the holes in the whole template. Then a drop of PMMA (4 wt%) was dropped on the sample to form a protecting layer, and the aluminum substrate was removed by placing the whole sample onto $CuSO_4$ solution (0.88 mol/L) for a night. After that, the bottom barrier layer of the AAO template was removed by placing the PMMA-protected template onto 0.3 M oxalic acid at a temperature of 45 ℃. Then the PMMA layer was dissolved by ace-

tone and the patterned AAO template was transferred onto a silica substrate. Lastly, the silver nanoparticles were deposited on the silica substrate by electron beam evaporation (DE400, Wavetest) and the AAO template was removed by tapes to leave just the final color pattern on the substrate.

The AAO template right after the second anodization had pores with $D = 40$ nm, and the etching steps were used to provide pores with larger D [Fig. 3(a)(i)]. After the deposit of silver, the D distribution of pores in AAO was transferred to the silver nanoparticle array [Fig. 3(a)(ii)]. Figure 3(a)(iii) shows the image of a fabricated silver semi-ellipsoid nanoarray with a tilted observing angle of 45° in a scanning electron microscope (SEM). Figure 3(b) shows the camera picture of a fabricated color pattern prepared by the aforementioned method.

To exemplify the angle independence of the presented plasmonic color printing, we characterized the fabricated nanoarray in both spectral way and visual way. As shown by the example in Fig. 3(c), the reflective peak wavelength of the nanoarray, measured using unpolarized light source, had no distinct change when the incident angles were altered from 8° to 60°. This experimental proof of angle independence is consistent with the simulated results. Accordingly, the insets in Fig. 3(c) also show no distinct color change on the sample regarding different observing angles. Also being consistent with the simulation, the reflective peak wavelengths and the corresponding colors were tuned from the blue region to the red region by applying different structural parameters [Fig. 3(d)]. Figure 3(e) gives the camera pictures of a fabricated color pattern at different observing angles, showing angle-independent colors up to 60°.

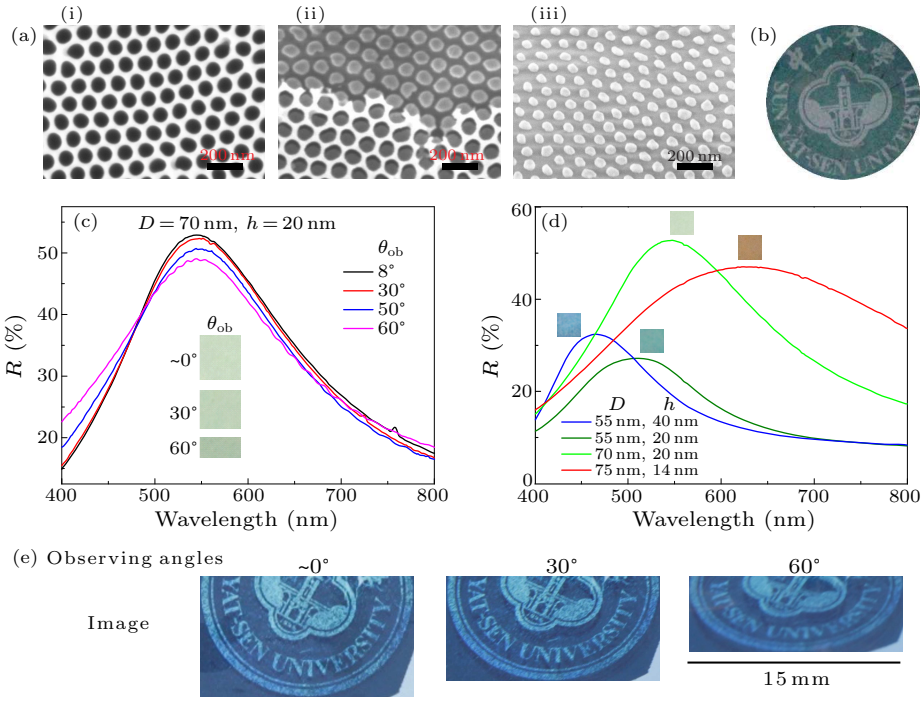

Fig. 3. Experimental demonstration of the angle-independent plasmonic color printing. (a) Scanning electron microscope images of the prepared samples. (i) The AAO template with enlarged holes. (ii) The fabricated semi-ellipsoid nanoarray with a part of the AAO template left. (iii) The semi-ellipsoid nanoarray observed at a tilted angle of 45°. The period of the nanoarray was fixed at 110 nm by the constant voltage used in the fabricating process. (b) A color pattern produced by the semi-ellipsoid nanoarray. (c) The measured reflection spectra of a silver semi-ellipsoid nanoarray with $D = 70$ nm and $h = 20$ nm regarding different incident angles from 8° to 60°. Inset: The camera pictures of the corresponding sample captured at the observing angles of ∼0°, 30° and 60°, respectively. (d) Measured reflection spectra of the four representative samples of the semi-ellipsoids nanoarray with reflective peak wavelengths ranging from blue region to red region of visible spectra. (e) The camera pictures of a fabricated color pattern captured at the observing angles of ∼0°, 30° and 60°, respectively. The reflection spectra and camera pictures are acquired under illumination of unpolarized light source.

The presented angle-independent plasmonic color printing can be used to construct flexible color printing. Unlike nano-gratings[19] or Fabry–Pérot structures,[42,49] our nanoarray consists of discrete nanoparticles, which means that there would be no harm to the structure when the substrate becomes flexible and is bent. As shown in Fig. 4(a), we fabricated a 15-mm badge on a flexible PDMS (i.e., polydimethylsiloxane) substrate, which can be bent without affecting the performance of the color prints.

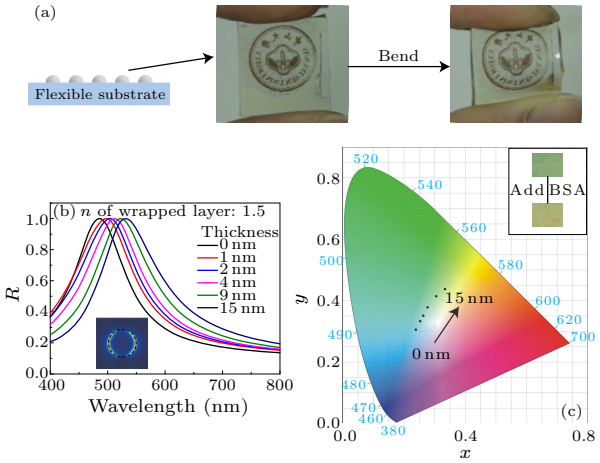

Fig. 4. Flexibility and potential applications in visualized bio-detection. (a) Flexible plasmonic color printing. (i) Schematic of the strategy for achieving flexibility by fabricating the color print on a flexible substrate. (ii) and (iii) The camera picture of a plasmonic color pattern fabricated on a PDMS substrate, in normal state (ii) and in bent state (iii). (b) The simulated reflection spectra of a silver semi-ellipsoid nanoarray with $D = 60$ nm, $h = 40$ nm and $P = 110$ nm, wrapped by a dielectric layer with thickness ranging from 0 to 15 nm. Inset: the simulated electric field distribution around a particle in the semi-ellipsoid nanoarray. The simulated plain is the surface of the substrate. (c) The CIE xy color co-ordinates corresponding to spectra in (b), showing the color shifts caused by the wrapped dielectric layer.

The presented approach of angle-independent plasmonic color printing also holds the potential for visualized bio-detection. The nanoarray has strong electric field enhancement effect near the surfaces of its unit nanoparticles, as shown by the inserted electric field distribution in Fig. 4(b). Therefore, the optical responses of the nanoarray would be sensitive to the change of the local refractive index near the nanoparticles. Figure 4(b) shows the spectral shift of a nanoarray ($D = 60$ nm, $h = 40$ nm) when the outer surfaces of the unit nanoparticles are wrapped by a dielectric layer ($n = 1.5$) with different thicknesses from 0 nm to 15 nm. It is demonstrated that the reflective peak wavelength of the nanoarray has a shift of 11 nm (from 486 nm to 497 nm) when the structure is covered by just 1 nm of the dielectric layer, and a spectral shift of 45 nm can be achieved with a 15 nm dielectric coating. Figure 4(c) transfers these spectral features into a CIE xy color space, showing distinct color transitions resulting from the wrapping of the dielectric layer. Therefore, even only a single layer of bio-molecules may cause substantial color change on the presented plasmonic color printing, constructing the basis for visualized bio-detection. As a preliminary experimental attempt, the inset in Fig. 4(c) shows the distinct color transformation after a sample was covered by bovine serum albumin (BSA) molecules (the sample was immersed in solution of BSA molecules for an hour, and then dried by N_2 after being rinsed in water). When the visualized bio-detection is fulfilled in the future, although the preparation part of conduction may be the same as conventional plasmonic bio-detection,[50] the readout of result can be performed simply by the naked eyes, which would greatly simplify the detection processes and may be used at remote areas without electricity.

In summary, we have demonstrated a feasible approach to achieve angle-independent plasmonic color printing. In the presented approach, silver nano semi-ellipsoids were arranged into periodic arrays of hexagonal lattice with deep-subwavelength periods, which gives rise to angle-independent colors with high reflectivity. The angle-independent plasmonic color printing is implemented by a scalable technique based on transfer of an anodized aluminum oxide template, and the as-prepared plasmonic color print keeps its colors unchanged even when the incident angle is up to 60°. In addition, we construct flexible plasmonic color printing based on the presented approach, and further demonstrate the potential of applying the angle-independent plasmonic color printing in visualized bio-detection. Our study not only provides a feasible way to address the angle-dependent issue of plasmonic color printing, but also shed light on its way to functionalization, boosting this field on its commercializing process for real-world applications.

References

[1] Schuller J A, Barnard E S, Cai W, Jun Y C, White J S and Brongersma M L 2010 *Nat. Mater.* **9** 193
[2] Ozbay E 2006 *Science* **311** 189
[3] Zhou Z K, Liu J, Bao Y, Wu L, Png C E, Wang X H and Qiu C W 2019 *Prog. Quantum Electron.* **65** 1
[4] Panoiu N C, Sha W E I, Lei D Y and Li G C 2018 *J. Opt.* **20** 083001
[5] Laux E, Genet C, Skauli T and Ebbesen T W 2008 *Nat. Photon.* **2** 161
[6] Ozaki M, Kato J and Kawata S 2011 *Science* **332** 218
[7] Liu Y J, Si G Y, Leong E S, Xiang N, Danner A J and Teng J H 2012 *Adv. Mater.* **24** OP131
[8] Kumar K, Duan H, Hegde R S, Koh S C, Wei J N and Yang J K 2012 *Nat. Nanotechnol.* **7** 557
[9] Graydon O 2015 *Nat. Photon.* **9** 487
[10] Kristensen A, Yang J K W, Bozhevolnyi S I, Link S, Nordlander P, Halas N J and Mortensen N A 2017 *Nat. Rev. Mater.* **2** 16088
[11] Goh X M, Zheng Y, Tan S J, Zhang L, Kumar K, Qiu C W and Yang J K 2014 *Nat. Commun.* **5** 5361
[12] Roberts A S, Pors A, Albrektsen O and Bozhevolnyi S I 2014 *Nano Lett.* **14** 783
[13] Tan S J, Zhang L, Zhu D, Goh X M, Wang Y M, Kumar K, Qiu C W and Yang J K 2014 *Nano Lett.* **14** 4023
[14] Xue J, Zhou Z K, Wei Z, Su R, Lai J, Li J, Li C, Zhang T and Wang X H 2015 *Nat. Commun.* **6** 8906
[15] Miyata M, Hatada H and Takahara J 2016 *Nano Lett.* **16** 3166
[16] Yang B, Liu W, Li Z, Cheng H, Choi D Y, Chen S and Tian J 2019 *Nano Lett.* **19** 4221
[17] Yang W, Xiao S, Song Q, Liu Y, Wu Y, Wang S, Yu J, Han J and Tsai D P 2020 *Nat. Commun.* **11** 1864

[18] Yang B, Liu W, Li Z, Cheng H, Chen S and Tian J 2018 *Adv. Opt. Mater.* **6** 1701009
[19] Zhang F, Pu M, Gao P, Jin J, Li X, Guo Y, Ma X, Luo J, Yu H and Luo X 2020 *Adv. Sci.* **7** 1903156
[20] Rezaei S D, Hong Ng R J, Dong Z, Ho J, Koay E H H, Ramakrishna S and Yang J K W 2019 *ACS Nano* **13** 3580
[21] Xiong K, Emilsson G, Maziz A, Yang X, Shao L, Jager E W and Dahlin A B 2016 *Adv. Mater.* **28** 9956
[22] Franklin D, Frank R, Wu S T and Chanda D 2017 *Nat. Commun.* **8** 15209
[23] Duan X and Liu N 2018 *ACS Nano* **12** 8817
[24] Peng J, Jeong H H, Lin Q, Cormier S, Liang H L, De Volder M F L, Vignolini S and Baumberg J J 2019 *Sci. Adv.* **5** eaaw2205
[25] Zhu X, Vannahme C, Hojlund-Nielsen E, Mortensen N A and Kristensen A 2016 *Nat. Nanotechnol.* **11** 325
[26] Murthy S, Pranov H, Feidenhans'l N A, Madsen J S, Hansen P E, Pedersen H C and Taboryski R 2017 *Nanoscale* **9** 14280
[27] Zhang Y, Zhang Q, Ouyang X, Lei D Y, Zhang A P and Tam H Y 2018 *ACS Nano* **12** 9913
[28] Xue J, Zhou Z K, Lin L, Guo C, Sun S, Lei D, Qiu C W and Wang X H 2019 *Light: Sci. & Appl.* **8** 101
[29] Liu H, Xu J, Wang H, Liu Y, Ruan Q, Wu Y, Liu X and Yang J K W 2019 *Adv. Mater.* **31** 1807900
[30] Franklin D, Chen Y, Vazquez-Guardado A, Modak S, Boroumand J, Xu D, Wu S T and Chanda D 2015 *Nat. Commun.* **6** 7337
[31] Fang Z, Xu H, Zheng Y, Chen Y and Zhou Z K 2020 *Chin. Phys. Lett.* **37** 077801
[32] Alrasheed S and Di Fabrizio E 2018 *Nanomater. Nanotechnol.* **8** 184798041877240
[33] Wu Q J, Jia H, Hu X L, Sun L B, Wang L S, Yang S M, Tai R Z, Fecht H J, Wang L Q, Zhang D X and Jiang J Z 2017 *Nanotechnology* **28** 085203
[34] Siddique R H, Mertens J, Holscher H and Vignolini S 2017 *Light: Sci. & Appl.* **6** e17015
[35] Wang H, Wang X, Yan C, Zhao H, Zhang J, Santschi C and Martin O J F 2017 *ACS Nano* **11** 4419
[36] Chen T and Reinhard B M 2016 *Adv. Mater.* **28** 3522
[37] Farjadpour A, Roundy D, Rodriguez A, Ibanescu M, Bermel P, Joannopoulos J D, Johnson S G and Burr G W 2006 *Opt. Lett.* **31** 2972
[38] Palik E D 1998 *Handbook of Optical Constants of Solids* (Boston: Academic Press)
[39] Elbahri M, Abdelaziz M, Homaeigohar S, Elsharawy A, Keshavarz Hedayati M , Roder C, El Haj Assad M and Abdelaziz R 2018 *Adv. Mater.* **30** 1704442
[40] Wang W, Ramezani M, Väkeväinen A I, Rivas J G and Odom T W 2018 *Mater. Today* **21** 303
[41] Liu S D, Yue P, Zhang S, Wang M, Dai H, Chen Y, Nie Z Q, Cui Y, Han J B and Duan H 2020 *Adv. Opt. Mater.* **8** 1901109
[42] Shaltout A M, Kim J, Boltasseva A, Shalaev V M and Kildishev A V 2018 *Nat. Commun.* **9** 2673
[43] James T D, Mulvaney P and Roberts A 2016 *Nano Lett.* **16** 3817
[44] Cetin A E, Etezadi D, Galarreta B C, Busson M P, Eksioglu Y and Altug H 2015 *ACS Photon.* **2** 1167
[45] Hao Q, Huang H, Fan X, Hou X, Yin Y, Li W, Si L, Nan H, Wang H, Mei Y, Qiu T and Chu P K 2017 *Nanotechnology* **28** 105301
[46] Hao Q, Huang H, Fan X, Yin Y, Wang J, Li W, Qiu T, Ma L, Chu P K and Schmidt O G 2017 *ACS Appl. Mater. & Interfaces* **9** 36199
[47] Masuda H and Fukuda K 1995 *Science* **268** 1466
[48] Li A P, Müller F, Birner A, Nielsch K and Gösele U 1998 *J. Appl. Phys.* **84** 6023
[49] Xiong K, Tordera D, Emilsson G, Olsson O, Linderhed U, Jonsson M P and Dahlin A B 2017 *Nano Lett.* **17** 7033
[50] Gerardo A L, Estevez M C, Maria S and Laura M L 2017 *Nanophotonics* **6** 123